

# VisTR: Visualizations as Representations for Time-series Table Reasoning

Jianing Hao, Zhuowen Liang, Chunting Li, Yuyu Luo, Jie Li, and Wei Zeng *Member, IEEE*

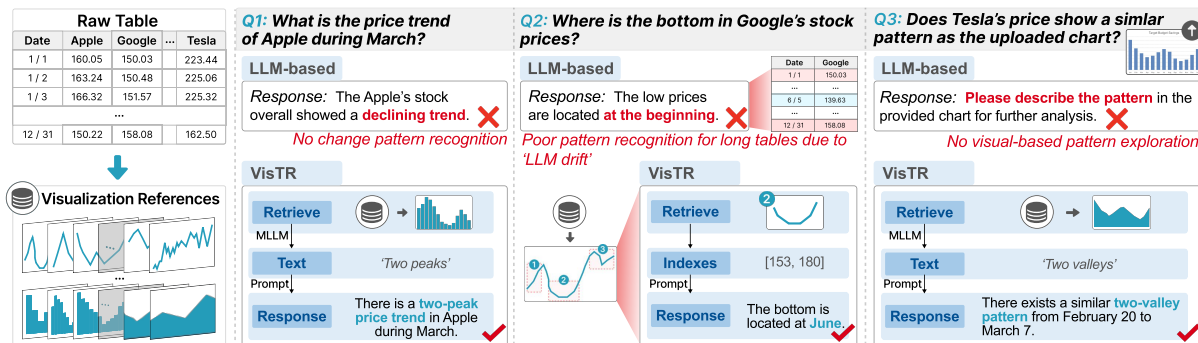


Fig. 1: *VisTR* leverages visualizations as the *representations* between a table and user intentions. The proposed framework advances existing LLM-based table reasoning methods by supporting data change pattern recognition (Q1), improving pattern recognition for long tables (Q2), and enabling visual-based pattern exploration (Q3).

**Abstract**— Table reasoning involves transforming natural language questions into corresponding answers based on the provided data table. Recent research exploits large language models (LLMs) to facilitate table reasoning, which however struggle with pattern recognition and lack support for visual-based pattern exploration. To address these limitations, we propose *VisTR*, a framework that leverages visualizations as *representations* to facilitate data pattern recognition and support cross-modal exploration. We describe *VisTR* as a process consisting of four major modules: 1) visualization alignment that utilizes multimodal LLMs to align visualizations across various modalities, including chart, text, and sketch; 2) visualization referencing that decomposes a table into multifaceted visualization references that comprehensively represent the table; 3) visualization pruning that incorporates data and retrieval pruning to excise visualization references with poor information and enhance retrieval efficiency; and 4) visualization interaction that offers an interactive visual interface with multimodal interactions for user-friendly table reasoning. Quantitative evaluation with existing multimodal LLMs demonstrates the effectiveness of the alignment model in cross-modal visualization pairings. We further illustrate the applicability of the proposed framework in various time-series table reasoning and exploration tasks.

**Index Terms**—Table reasoning, visualization representation, multimodal LLMs

## 1 INTRODUCTION

Table reasoning is a crucial natural language processing task that involves automatically extracting and inferring information from tables to answer specific questions [12, 70]. This task supports a wide range of applications such as fact verification [6] and question answering [26], where each question-table pair constitutes an instance for reasoning [69]. Given the superior commonsense and logical reasoning capabilities of large language models (LLMs) [63], utilizing them for table reasoning has emerged as the predominant approach [5, 12]. Existing methods can be broadly categorized into *generic table reasoning*, where pre-trained models or LLMs directly generate answers, often enhanced by techniques such as designing prompts [5] to guide iterative reasoning or employing flexible tabular formats [57, 69]; and *program-aided table reasoning* that utilizes executable query languages

(e.g., SQL, SPARQL, or Python) as the bridge between user queries and answers derived from the table [9, 19, 65].

Despite their advancements, there exist several limitations. First, these methods struggle with pattern recognition, which involves the automatic identification and extraction of meaningful patterns within data, such as trends in time-series data [8, 35]. For instance, Q1 in Figure 1 illustrates a scenario where users seek to examine the price trend of Apple during March. Existing LLM-based methods cannot correctly capture and respond to the data change patterns within the corresponding time period. The challenge becomes more pronounced when dealing with large-size tables, as LLMs are known to encounter ‘drift’ issues, where models lose information in the middle of long contexts [4]. This loss of context can result in errors during the reasoning process, making it difficult to extract patterns accurately, as illustrated in Figure 1(Q2). Last, the methods lack support for visual-based pattern exploration, making it challenging for users to iteratively engage with data tables, particularly for lay users. Rather than expressing their intentions precisely in natural language, laymen would prefer to use multimodal inputs like hand-drawn sketches or charts [41]. An example is shown in Figure 1(Q3), where a user may not know the term “two-valley” but can easily recognize this visual pattern from the collected bar chart. However, existing LLM-based methods do not support such visual-based exploration, which are increasingly in demand.

To overcome the limitations of existing LLM-based table reasoning methods, we introduce a novel framework that incorporates visualization as *representation* into multimodal LLMs (MLLMs). Our **key idea** is to transform *data tables* into a set of meaningful and insightful visualizations, termed *visualization references*, which serve as a concise data *representation* to capture data insights and align with human intentions.

arXiv:2406.03753v2 [cs.LG] 20 Nov 2024

- J. Hao, C. Li, Y. Luo and W. Zeng are with the Hong Kong University of Science and Technology (Guangzhou). Y. Luo and W. Zeng are also with the Hong Kong University of Science and Technology. E-mail: {jzhao768@connect., cli087@connect., yuyuluo@, weizeng@jhkust-gz.edu.cn.
- Z. Liang is with the South China University of Technology. simonliang484@gmail.com.
- J. Li is with the Tianjin University of Technology. jie.li@tju.edu.cn.

Manuscript received xx xxx. 201x; accepted xx xxx. 201x. Date of Publication xx xxx. 201x; date of current version xx xxx. 201x. For information on obtaining reprints of this article, please send e-mail to: [reprints@ieee.org](mailto:reprints@ieee.org). Digital Object Identifier: xx.xxxx/TVCG.201x.xxxxxx

This framework offers several advantages that address the shortcomings of existing LLM-based table reasoning methods, effectively enhancing the table exploration process. First, visualization references can help recognize the short- and long-term data change patterns. For instance, when recognizing price trend in the given data table (Figure 1(Q1)), the corresponding visualization reference could capture the “two-peak” price trend of Apple during March. Second, regardless of the length of data facets, the visualization references can capture and retain the data change patterns in fixed-size images. Adopting fixed-size visualization references as the representations of data facets can effectively circumvent the ‘drift’ issues encountered during reasoning. For Q2 in Figure 1, the stock price change over a year can be represented as a single visualization, where the price bottom can be easily located in this reference. Moreover, leveraging visualizations as a *representation* offers new modalities for interacting with the tabular data, aligning more intuitively with human intentions [32]. Combined with multimodal input, including text and chart (as shown in Figure 1(Q3)), it becomes easier to explore data tables than directly observing the raw table.

We illustrate the effectiveness of *VisTR* on time-series data tables, which often feature large table sizes and complex data change patterns. In this context, the proposed framework also presents several challenges to be addressed. First, time-series data often contain a variety of long- and short-term patterns, which should be comprehensively captured by the visualization references. To ensure the visualization references are comprehensive enough to accurately represent a data table, thereby meeting the diverse analytical needs, poses the first challenge (C1). Second, to effectively align textual descriptions, visualization images, and hand-drawn sketches to bridge user intentions with visualization references, meanwhile enabling multimodal interactions presents a challenge (C2). Existing models for vision-language tasks such as chart question answering (CQA) [24, 68] are not specifically designed to meet this requirement, thus being less effective in identifying data change patterns. Last, to comprehensively represent a table, a large number of visualization references will be generated. Effectively indexing the visualization references and supporting efficient visualization retrieval for timely user response present a significant challenge (C3).

We design a prototype system that encompasses four main modules aimed at addressing the challenges C1–C3. First, the *visualization referencing* module decomposes an input table into data facets and processes the facets into corresponding visualization references that comprehensively capture the essence of the table. To ensure a comprehensive representation of data patterns in tabular data, we adopt a multifaceted process to get meaningful facets and then transform each facet into a fixed-size visualization reference (*addressing C1*). Second, in the *visualization alignment* module, we fine-tune a MLLM to connect visualizations of various modalities including charts, text, and sketches (*addressing C2*). Specifically, we construct a new cross-modal visualization dataset using data augmentation for chart-text pairing and user labeling for chart-sketch pairing, taking into account user intentions. We further leverage the CLIP model [48] enriched with two-level cross-entropy loss and bidirectional hinge-based triplet ranking loss to enhance the alignment. Next, the *visualization pruning* module leverages visualization pruning to filter out less informative visualization references, and visualization indexing to enhance the efficiency of the retrieval process for the embeddings of visualization references stored in a vector database (*addressing C3*). Finally, we design a *visualization interface* that enables users’ exploration of time-series data tables through multimodal interactions. Here, we incorporate a “decomposing-execution-filling” strategy to integrate the output generated by *VisTR* with the input table. Specifically, the user input is initially decomposed into visualization retrieval tasks, which are executed in the vector database, and their corresponding text descriptions are extracted by the fine-tuned MLLM. Subsequently, these descriptions are filled back into the input table to generate textual responses for the user. Quantitative evaluations demonstrate the effectiveness of the fine-tuned MLLM in aligning different modalities. Additionally, case studies illustrate how the proposed framework addresses the limitations of existing LLM-based table reasoning methods through various time-series table reasoning and visual-based exploration tasks. Dataset, fine-tuned model,

and evaluation results are released at <https://osf.io/yun9d/>.

In summary, we make the following contributions:

- (1) **Framework.** We introduce a framework that leverages visualizations as the *representations* to enhance table reasoning, to facilitate data change pattern recognition and visual-based exploration.
- (2) **Multimodal Visualization Alignment.** We design an effective MLLM that learns a joint embedding space across three visualization modalities - charts, text, and hand-drawn sketches. The model aligns multimodal user intentions with visualization references, allowing users to explore and analyze tables through various interactions.
- (3) **VisTR System.** We develop a prototype system that supports the exploration and reasoning of large-scale and multiple time-series tables through intuitive user interactions. Various case studies and quantitative results prove the effectiveness and applicability of *VisTR*.

## 2 RELATED WORK

**Table Reasoning.** Table reasoning integrated with natural language (NL) interfaces enables lay users to explore tabular data effortlessly, supporting complex tasks such as fact verification [6] and question answering [26]. Existing LLM-based table reasoning methods can be categorized into *generic table reasoning* and *program-aided table reasoning* [57]. Generic reasoning methods employ LLMs to interpret and respond to free-form NL queries by generating answers directly from tables [5]. However, due to the complexity of table structure, these methods struggle with large tables and offer limited explainability because of their end-to-end nature. Program-aided table reasoning utilizes executable query languages, such as SQL, to form a structured and accountable bridge between user queries and the derived answers [14, 25, 37]. Recent research has mostly focused on leveraging LLMs to transform complex user utterances into SQL queries with data context awareness [65], using prompt engineering [30], chain-of-thought [57, 66], and pre-training techniques [56]. However, program-aided approaches encounter intricate limitations due to their reliance on query language. First, SQLs primarily cater to numerical queries from tables but lack support of analytical functionality [29], overlooking data change patterns. Second, when confronted with large tables, LLMs may encounter drift issues [4] while accessing information in the middle of long contexts. Moreover, in many scenarios, relying solely on textual inputs limits the expression of non-verbal intentions, such as hand-drawn sketches, reducing the flexibility of user interactions.

To overcome these limitations, this work introduces a novel framework that leverages visualizations as a *representation* between tables and user intentions. Our inspiration is that visualizations can depict intuitive data patterns and illustrate complex underlying processes [18], aiding swift and effective interpretation by users [31]. However, this approach also presents challenges to be tackled. First, tabular data typically encompass numerous features, leading to a plethora of potential visualizations [54, 62] that complicate interactive interactions. Second, there are no direct approaches available to connect free-form user queries with visualizations.

**Multimodal Visualization Alignment.** Given that visualizations are inherently stored as images, we opt to leverage emerging MLLMs to embed visualization images and facilitate multimodal user interactions. In recent years, significant advancements have been made in utilizing vision-language models for chart-based tasks, such as CQA [24, 42, 43], chart retrieval [60] and generation [50, 61]. Though CQA models can provide answers for user utterances, these models only support text-chart interactions, lacking the capability for cross-modal interactions involving multiple modalities such as text, chart, and sketch preferred by laymen. Furthermore, these models are not specifically designed for effectively recognizing data change patterns (see Sect. 6.1), a gap that this work seeks to fill in the context of table reasoning.

To this end, we choose to construct a novel vision-language model with an innovative visualization alignment strategy. Most existing multimodal data alignment methods rely on contrastive language-image pre-training (CLIP) [48], which has demonstrated its adaptability and proficiency across various tasks [34, 71, 72], highlighting the effec-

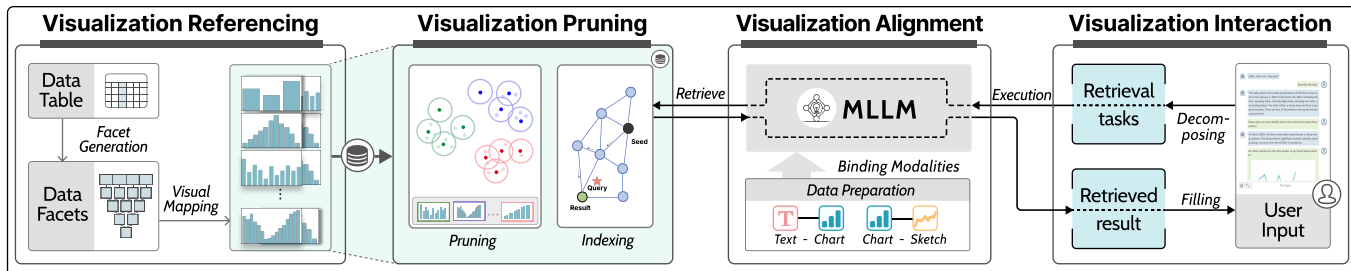


Fig. 2: An overview of the proposed framework, which mainly contains four main modules of *visualization referencing*, *visualization pruning*, *visualization alignment*, and *visualization interaction*.

tiveness of joint embedding spaces. However, training an effective CLIP-based alignment model for visualizations is non-trivial. First, this task involves aligning more than two modalities, including text, hand-drawn sketches, and various types of charts, whereas the original CLIP model was designed to support text-image alignment. To encompass more modalities, we adopt joint embedding strategies that leverage charts as naturally aligned supervision and emergent alignments to unify other modalities [20]. This approach allows us to prepare paired data only for chart-text and chart-sketch, rather than other pairings such as sketch-text. Second, the effectiveness of CLIP is largely attributed to its extensive training on vast (natural) image-text datasets, whereas there is a lack of suitable training datasets for the task in this work. Efforts have been made to construct datasets for promoting deep learning models for chart-text (e.g., [28, 42]), chart-chart (e.g., [33, 40, 64]), chart-sketch (e.g., [38, 41, 52]) similarity measurement. However, these different modalities are not inherently unified in one model, and many of these datasets are not specifically designed for recognizing data change patterns. To address this gap, we utilize data augmentation and user labeling strategies to supplement existing datasets in training the multimodal visualization alignment model.

**Visualization Storage, Indexing, and Retrieval.** To comprehensively represent tabular data, our approach will generate a large number of visualization references and encode them into vector representations, thus raising new challenges for efficiently storing, indexing, and retrieving them. With the recent advancements in Vector Database Management Systems (VDBMS) [46], there is potential to meet our demand. VDBMSs are specifically designed for managing high-dimensional data, such as embeddings, offering sophisticated storage, indexing, query processing, and query optimization capabilities [3]. Their ability to perform efficient similarity searches in high-dimensional spaces makes them particularly suited for tasks involving the retrieval of embeddings based on content or semantic similarity. This supports various applications such as information retrieval, e-commerce, and recommendation platforms [22, 55]. Existing VDBMS can be roughly categorized into two types: *native* systems and *extended* systems [46]. The former, such as Chroma [1] and EuclidesDB [2], are tailored for vector data management, while the latter, such as AnalyticDB-V [58], are built on top of an existing data management system.

In this work, we first introduce a visualization pruning method to filter out less informative visualizations, and effectively reduce storage demands while maintaining the quality of stored visualizations. We then integrate Chroma [1] into *VisTR* and utilize an efficient graph-based index to store and index the large collection of visualization references. An *Approximate k-Nearest Neighbors* (ANN) algorithm is incorporated to retrieve visualizations. The combination of pruning with indexing allows for quick retrieval and handling timely user queries.

### 3 THE VISUALIZATION ENHANCED FRAMEWORK

The visualization enhanced framework consists of four modules: *visualization alignment*, *visualization referencing*, *visualization pruning*, and *visualization interaction*, as shown in Figure 2.

**Visualization Alignment.** As the cornerstone of our framework, a MLLM is fine-tuned to establish a single joint embedding space for various modalities, including chart (C), text (T), and sketch (S). To address the issue of a lack of suitable training data, we first curate a new

dataset with chart-text pairings augmented from existing Chart-to-Text dataset [28], and chart-sketch pairings through user labeling. Utilizing the pre-trained CLIP [48], we fine-tune a multimodal LLM on our composite dataset, employing a Transformer [49] for text modality, and ViT [13] encoders for chart and sketch modalities, respectively. To achieve alignment across modalities within the joint embedding space, we implement a bidirectional hinge-based triplet ranking loss function and a two-level cross-entropy loss function. Through this process, we successfully align the three modalities and yield strong performance across four evaluation metrics surpassing a threshold of 0.85. A detailed description of the module is provided in Sect. 4.

**Visualization Referencing.** In the *visualization referencing* module, we generate visualization references that comprehensively capture key data patterns inherent in an input table. This module employs a two-stage approach that first decomposes the input table  $D$  into data facets, which are then mapped into fixed-size visualization references. The description of this module is detailed in Sect. 5.1.

**Visualization Pruning.** In the *visualization pruning* module, we introduce pruning and indexing techniques to enable timely visualization reference retrieval. Specifically, visualization pruning works by filtering out less informative visualization references by measuring the similarity between visualization vectors using Euclidean distance and applying a pruning threshold. This process reduces the number of stored references while preserving essential data change patterns. Concurrently, visualization indexing leverages an open-source vector database, Chroma [1], to efficiently store and retrieve visualization references. Here, we use the fine-tuned MLLM to transform all the pruned visualization references into 512-dimensional vectors, which are then indexed by Chroma for rapid and accurate follow-up retrieval. This combination of pruning and indexing ensures *VisTR* can swiftly manage and retrieve massive visualization references with precision. This module is detailed in Sect. 5.2.

**Visualization Interaction.** In the *visualization interaction* module, we introduce a “decomposing-execution-filling” strategy to enable the connection of multimodal user queries with the stored embeddings of visualization references. Specifically, the user query is first decomposed into a visualization retrieval task. Second, the retrieval task is executed in Chrome to get a retrieved visualization reference. Afterward, with the help of the fine-tuned MLLM, the corresponding trend word of the retrieved visualization reference is generated and then filled into the textual response to the user. An interactive visual interface with multiple views and rich interactions is also developed to support the iterative table reasoning process, transitioning from abstract to detailed exploration, as detailed in Sect. 5.3.

### 4 MULTIMODAL VISUALIZATION ALIGNMENT

We set out to establish a MLLM that aligns visualization modalities of chart, sketch, and text in a single joint embedding space. This section presents the data preparation, including data augmentation and user labeling strategies, to address the issue of lacking training dataset (Sect. 4.1), followed by modality binding for establishing a joint embedding space that binds chart, sketch, and text modalities together (Sect. 4.2). In the end, we present the implementation details (Sect. 4.3).

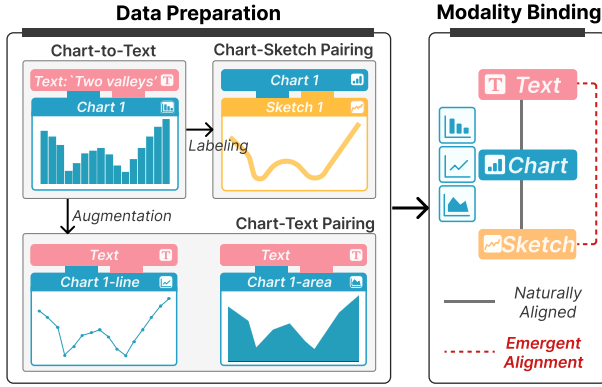


Fig. 3: An overview of *visualization alignment* module, which contains data preparation for chart-text and chart-sketch pairings, and achieves the alignment for chart, sketch, and text modalities.

#### 4.1 Data Preparation

To train the multimodal visualization alignment model, we need to first prepare a dataset containing user intentions, which is not covered by current open-sourced datasets. To achieve the alignment of sketches, charts, and text, we employ two strategies to construct the training data: (1) data augmentation for chart-text pairing, and (2) user labeling for chart-sketch pairing. Figure 3 uses an example to illustrate the two data preparation strategies.

(1) **Data augmentation for chart-text pairing.** To make up for the lack of data change pattern recognition in the existing table reasoning works, we should focus on the charts that describe data change patterns. We first survey existing chart-text datasets, and find that different textual contents are contained for different downstream tasks. We select the Chart-to-Text dataset [28] as the original dataset because it offers textual descriptions and underlying data tables for charts. Since we mainly focus on the data change patterns existing in charts, we filter the trend words from the textual descriptions. Initially, we manually extracted the contained trend words in five textual descriptions. These five descriptions with their corresponding trend words served as prompts for GPT-4 to perform an accurate trend word filtering process on the large Chart-to-Text dataset. In the filtering process, we find diversity in both trend words and charts. For trend words, we notice that different trend words in textual descriptions may indicate the same change pattern, such as ‘increasing’, ‘upward’, and ‘rising’, which typically indicate an upward trend in the data. We construct a dictionary of similar trend words, grouping the words describing similar patterns into the same category, and we get 23 categories ( $N_T = 23$ ) of trend words. For charts, we find that three chart types: line, bar, and area charts, are widely chosen to describe the data change patterns. To balance the number of three chart types contained in the final chart-text pairing dataset, we supplement each filtered chart with two other types of charts. In total, we create a total of 5,010 chart-text pairings.

(2) **User labeling for chart-sketch pairing.** When searching for hand-drawn sketch datasets associated with charts, we encounter a significant challenge: existing public sketch datasets do not adequately meet our need to convey users’ intentions about data change patterns. Specifically, the existing sketch datasets are not suitable for our work due to the following points. 1) Most open-sourced large human sketch datasets *e.g.*, [15], mainly focus on how users draw objects, rather than on visualizations. 2) LADV [39] and VisAtlas [64] are designed for chart type matching based on pixel-wise similarity, but not the contained data change patterns. 3) Sketch query systems, such as Qetch [41], focus on data-level similarities between hand-drawn sketches and the raw data, which lacks correspondence with fixed-size charts.

In order to collect chart-sketch pairings that conform to users’ intentions about data change patterns, we invite users to draw sketches and evaluate chart-sketch pairings. 1) *Setup.* Every user is given a training session to get familiar with experimental procedures and hand-drawn board operations. 2) *Reference chart selection.* Every user is given 100 real charts selected from our chart-text pairing dataset. The selected

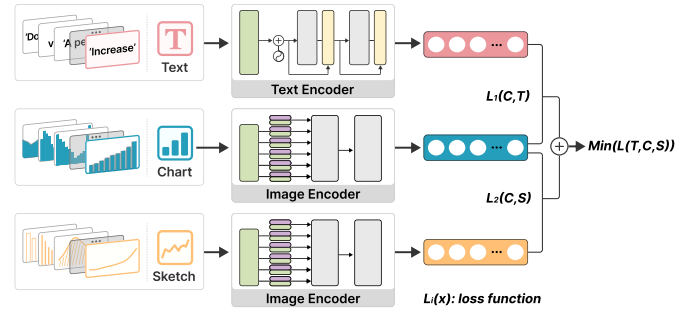


Fig. 4: The alignment pipeline for three modalities. Each modality is processed by a separate encoder, and the chart modality is set as the supervisor, guiding the alignment process.

charts cover 23 categories of trend words, and contain bar, line, and area charts. 3) *Drawing.* The selected charts are displayed to the user one by one, and the user draws a sketch, which he/she thinks represents the change patterns in the displayed chart on the free-scale board. 4) *Evaluation/Redraw.* After drawing all the given charts, we show them the sketch with the corresponding chart one by one, and the user could delete or redraw the sketches they are not satisfied with. A total of 10 users (six women, four men) aged from 18 to 30 were invited. They all have knowledge of data visualization and are experienced in drawing sketches. In the end, we filter low-quality sketches, resulting in 1,214 pairs of chart-sketch pairings ready for training.

#### 4.2 Modality Binding

We aim to bind all text  $T$ , chart  $C$  and sketch  $S$  modalities together in a joint embedding space. Existing CLIP-based works predominantly focus on aligning pairs of modalities, while our objective is to accomplish the alignment of three modalities in the absence of the pairings between text and sketch modalities. As shown in Figure 4, we employ a two-stage strategy: first, we employ modality-specific encoders to transform each modality into embeddings of uniform length [59]. All three modalities are processed using the Transformer architecture, leveraging its self-attention mechanism to effectively capture complex dependencies within each modality.

Given a chart  $C_i$  with its corresponding observation  $T_i$  in text modality, and observation  $S_i$  in sketch modality, we encode them into normalized embeddings:  $p_i = f(C_i)$ ,  $q_i = f(S_i)$ , and  $k_i = f(T_i)$ , where  $f$  is a 63M-parameter 12-layer 512-wide Transformer with the architecture modifications with 8 attention heads [49] for text modality, and the Vision Transformer (ViT) [13] with a patch size of 32 for chart and sketch modalities. Each modality is processed by a separate encoder, which is designed to cater to the unique characteristics of the input. We add a modality-specific linear projection head on each encoder to obtain a fixed size  $d$  dimensional embedding, which is normalized, and set as  $p_i$ ,  $q_i$ , and  $k_i$  for loss calculation. Besides facilitating learning, this setup allows us to initialize a subset of the encoders with weights from pre-trained CLIP [48] models. This initialization not only provides a strong starting point for our MLLM but also enables it to better understand and align the semantic content across different modalities.

During the second stage, we combine the two-level cross-entropy and a bidirectional hinge-based triplet ranking loss to guide the three modalities to align in the latent space. We elect the chart modality,  $C$ , as the supervised modality because visualization references are in the form of charts, and the chart-text and chart-sketch pairings that span a wide range of change patterns are well collected. Inspired by VSE++ [16], we address this by introducing the two-level cross-entropy and a bidirectional hinge-based triplet ranking loss, which makes the matched pairs have smaller entropies than unmatched ones. The formulation for the two cross-entropy functions is specified as:

$$H_1(C, T) = -\sum(p_i \times \log(k_i)),$$

$$H_2(C, S) = -\sum(p_i \times \log(q_i)),$$

where  $H_1$  calculates the difference between charts  $C$  and text  $T$ , and  $(C, T)$  is the matched positive chart-text pair.  $H_2$  calculates the dif-

ference between charts  $C$  and sketches  $S$ , and  $(C, S)$  is the matched positive chart-sketch pair.

We consider the loss function for the chart-text pairings as  $L_1(C, T)$ , and the loss function for the chart-sketch pairings as  $L_2(C, S)$ . Take chart and sketch modalities as an example, the loss is as follows:

$$L_2(C, S) = [\alpha + H_2(C', S) - H_2(C, S)]_+ + [\alpha + H_2(C, S') - H_2(C, S)]_+,$$

where  $\alpha$  denotes the margin parameter, and  $[x]_+ \equiv \max(x, 0)$ .  $C' = \arg \max_{X \neq C} H_2(X, S)$  and  $S' = \arg \max_{Y \neq S} H_2(C, Y)$  denote the hardest negative corresponding to the positive pair  $(C, S)$ . The loss makes the chart embedding  $p_i$  and the sketch embedding  $q_i$  closer in the joint embedding space, and thus aligns  $\mathbb{C}$  and  $\mathbb{S}$ . Set  $L$  as the final loss of three modalities in the embedding space, that is, the sum of the two ranking losses:  $L(T, C, S) = L_1(C, T) + L_2(C, S)$ . By minimizing both the loss between chart and text modalities, and the loss between chart and sketch modalities, we achieve the alignment between the similar embeddings of the three modalities in a joint embedding space.

### 4.3 Implementation Details

We took a pre-trained CLIP text-image model and fine-tuned it on the selected chart-text and chart-sketch pairings. In the training phases, we employed a strategy where we froze the ViT encoder and conducted fine-tuning for 30 epochs with a batch size of 32, and a learning rate of  $1e^{-5}$ . The model parameters were optimized using AdamW optimizer, employing Betas (0.9, 0.98), weight decay of 0.001, and incorporating of StepLR learning rate schedule. This static scheduler ensures that the learning rate gradually decreases during fine-tuning, facilitating convergence towards a local optimum. Through using the modalities paired with charts, *i.e.*, pairs of the form  $(\mathbb{C}, \mathbb{T})$ , and  $(\mathbb{C}, \mathbb{S})$  to align each the embeddings from text modality  $\mathbb{T}$  and sketch modality  $\mathbb{S}$  to those from charts. We observe that the pairs  $(T, S)$  are aligned even though we only train using the pairs  $(C, T)$  and  $(C, M)$ . This behavior is also validated by IMAGEBIND [20] so we reference to its statement that  $(\mathbb{C}, \mathbb{S})$  and  $(\mathbb{C}, \mathbb{T})$  are naturally aligned, and the text  $\mathbb{T}$  and sketch modalities  $\mathbb{S}$  constitute an emergency alignment.

## 5 VisTR SYSTEM

With the MLLM for multimodal visualization alignment, we build *VisTR* system that allows users to intuitively explore, comprehend, and interact with tabular data using visualizations as the *representation*. This section details the implementation of *visualization referencing* (Sect. 5.1), *visualization pruning* (Sect. 5.2), and *visualization interaction* (Sect. 5.3) in *VisTR* system.

### 5.1 Visualization Referencing

This module is designed to ensure that the generated visualization references can effectively capture comprehensive data patterns inherent in the raw tabular data. To this end, we design a two-stage approach that first generates data facets to capture all underlying data change patterns and then maps all data facets into visualization references.

**Facet Generation.** In the first stage, we aim to capture meaningful data facets of the input table as comprehensively as possible. If we use violent enumeration, it will produce a lot of candidate data facets, and many of them will not include data trends. To avoid the inefficient data facet generation, we adopt the idea of subset embedding [62] indicating that patterns of multi-dimensional data are often related to subsets rather than records. Specifically, we adopt a multifaceted process that incorporates a dual strategy of smoothing and segmentation.

Consider an input time-series table  $D(\text{timestamp}, d_1, d_2, \dots, d_n)$ , where each  $d_i$  represents a distinct variable containing a sequence of data points indexed by the timestamp. The first step is to smooth each variable  $d_i$  to retain essential patterns while filtering out the noise. To achieve this, *VisTR* employs Gaussian Smoothing, a technique favored for maintaining shape consistency under the Fourier transform [53]. Formally, for each each variable  $d_i$ , the smoothed series  $\tilde{d}_i$  is obtained as:  $\tilde{d}_i = \text{GaussianSmoothing}(d_i)$ . Compared with widely used Moving Average (MA) or Weighted Moving Average (WMA) [23], Gaussian

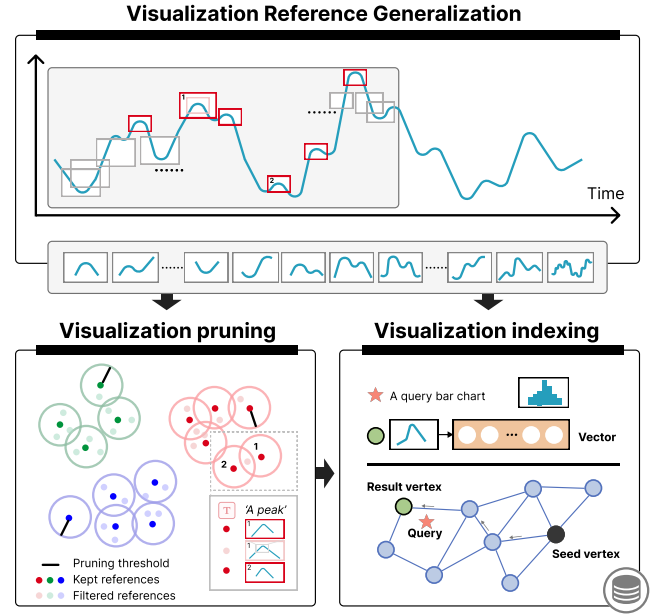


Fig. 5: The pipeline of *visualization referencing* and *visualization pruning* modules. Visualization pruning and indexing are used to accelerate the storage and retrieval process.

Smoothing can not only preserve key features while smoothing but also have flexibility in parameter control.

After smoothing, we segment each smoothed variable  $\tilde{d}_i$  into distinct facets to extract meaningful and reliable patterns. The segmentation process is defined as  $R(\tilde{d}_i) = \{r_1(\tilde{d}_i), r_2(\tilde{d}_i), \dots, r_m(\tilde{d}_i)\}$ , where  $r_j(\tilde{d}_i)$  represents a subset (termed as a facet) of  $\tilde{d}_i$ . To ensure each data facet reflects a valid data pattern, we incorporate the Page-Hinckley Test (PHT) [44] to detect critical points where shifts occur, thereby delineating the boundaries between different facets. Specifically, the segmentation process can be formalized as  $R(\tilde{d}_i) = \text{PHT}(\tilde{d}_i)$ . Additionally, we aggregate continuous subsets to form new facets, enabling the inclusion of segments with varying lengths.

**Visual Mapping.** The second stage is visual mapping, where we transform each data facet into a standard visual representation. This process leverages the *matplotlib* library to generate fixed-size visualization references devoid of axes, specifically utilizing bar, line, and area charts to manifest the trend within each data facet. The uniformity provided by fixed-size visualization references improves the fine-tuned MLLM's capacity to analyze and process them. For each data facet  $r_j(\tilde{d}_i) \in R(\tilde{d}_i)$ , the visual mapping process transforms  $r_j(\tilde{d}_i)$  into a fixed-size visualization reference  $c_j$ , which is formalized as  $c_j = \text{vmap}(r_j(\tilde{d}_i))$ . The collection of all visualization references derived from the data facets of a particular variable  $d_i$  is represented as  $C(d_i) = \{c_1, c_2, \dots, c_m\}$ . Collectively, for all variables in the input table  $D$ , the visualization references are denoted as  $C = \bigcup_{i=1}^n C(d_i) = \{c_{i,j} | d_i \in D, r_j(d_i) \in R(d_i)\}$ .

### 5.2 Visualization Pruning and Indexing

For a given table, we will generate a vast collection of visualization references, each of which is subsequently mapped into vector representations (*i.e.*, embeddings). The large number of visualization references poses significant challenges to efficient storage and retrieval. To address these challenges, we design a combined approach of visualization pruning and indexing, as illustrated in Figure 5, to improve *VisTR*'s ability to manage and retrieve visualization references.

**Visualization Pruning.** Here, the key idea is to filter out less informative visualization references in advance while retaining those that provide significant insights. The main challenge lies in discerning and preserving highly valuable visualization references during pruning. For all visualization references for a variable  $d_i$ , it may encounter a scenario where two references exhibit similar change patterns, and one is

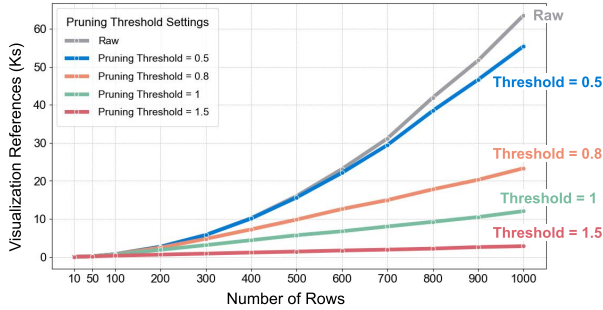


Fig. 6: The relationship between the number of visualization references, table rows, and the pruning threshold. The remaining visualization references are close to approximately 20% of the raw number when the pruning threshold is set to 1.

entirely encompassed by the other. We quantify the similarity between visualization vectors using the Euclidean distance  $d(c_j, c_k)$  between the two vectors  $c_j$  and  $c_k$ . We introduce a pruning threshold to determine whether two visualization vectors are sufficiently similar to warrant pruning. If  $d(c_j, c_k)$  is less than the set pruning threshold, the vector covering a shorter time range is filtered out. An example scenario is illustrated in Figure 5, where the ‘a peak’ change pattern exists in pink-boxed visualization references. In this case, the light-pink-boxed one has less information and is consequently filtered out.

The pruning threshold acts as a predefined parameter that affects the number of stored visualization references. To assess its impact, we designed an experiment with four values: 0.5, 0.8, 1, and 1.5, and applied the thresholds to tables in a range of row numbers. Specifically, the row numbers were considered based on the typical sizes used in existing LLM-based table reasoning methods, which typically support data tables with fewer than 50 rows. For instance, Tabfact [7], a commonly used dataset containing over 16k Wiki tables, has an average of 12.96 rows per table (max.=48, min.=1, std.=8.46). Given the focus on time-series data tables and long-term trend analysis, we extended the experiment to tables with up to 1000 rows, approximately encompassing four trading years. We calculated the average number of visualization references across three sub-tables with corresponding table sizes extracted from the DJI. data table for each pruning threshold.

Figure 6 shows the relationship between the number of stored visualization references, the number of data table rows, and the pruning thresholds. When the pruning threshold is set to 1, the number of stored visualization references approximated 20% of the raw reference number. This aligns with the well-known Pareto principle (80/20 rule) [45], which is widely leveraged in various optimization strategies to balance efficiency and information retention. As such, we also set the pruning threshold to be 1. This strikes a balance between maintaining a rich representation set and reducing the storage footprint.

**Visualization Indexing.** For efficient retrieval of visualization references, we utilize an open-sourced vector database named Chroma [1], which enables effective indexing and retrieval of embeddings. Specifically, we first apply our fine-tuned MLLM to encode all visualization references into 512-dimensional vectors. Chroma automatically maintains an index document when encoding all visualization references for retrieval. These indexes compress vectors into codes of a fixed size, storing them in an array. For similarity measurement, we employ the dot product function. By leveraging Chroma’s advanced indexing capabilities, *VisTR* efficiently speeds up the retrieval process to handle vast amounts of visualizations, ensuring both speed and accuracy.

### 5.3 Visualization Interaction

**The Decomposing-Execution-Filling Strategy.** Inspired by Dater [65], we introduce a ‘decomposing-execution-filling’ strategy to decompose and parse multimodal user queries and return results that meet user expectations. Specifically, we first decompose a user’s table reasoning queries and convert them into visualization reference retrieval operations, similar to text-to-SQL parsing (e.g., [47, 56]). Afterward, we execute the visualization retrieval operations in Chroma and get the

result for back-filling the final response.

Here, we employ two LLMs with in-context learning using prompts to decompose user queries and complete outputs respectively. Below we illustrate an example using the case shown in Figure 1(A). Given the query “What is the price trend of Apple during March?”, we first decompose the question into a retrieval task “return the visualization reference of Apple price in March”, and a cross-modal alignment task “recognize the trend in the retrieved visualization reference”. The corresponding visualization reference is first retrieved from Chroma, and then aligned with the ‘two peaks’ pattern to generate the final textual response “There is a two-peak price trend in Apple during March.”. Detailed prompts are provided in our open-sourced code.

**Visual Interface.** In addition to textual responses, *VisTR* also incorporates a user-friendly interface to enable intuitive table reasoning and exploration. As shown in Figure 7, the interface includes four main views: (A) Data Table, (B) Main View, (C) Chat Box, and (D) Pattern View. When a user uploads a table, the back-end of *VisTR* processes the tabular data into visualization references and stores them in the vector database, while the front-end interface displays the uploaded table in Data Table, and presents the visualization for the data in the Main View. By default, Main View uses an area graph for the overall context information and a line chart for the details. Various operations, such as selecting different variables or combinations of variables to display, are enabled in the drop-down box in the upper right corner of Main View. For the display of multi-variables, we use a multi-line chart with colors to encode different variables. The bottom area chart also allows for fixed-scale zooming and brushing, allowing users to observe detailed variable changes.

The Chat Box provides a dialogue window that supports multi-round conversations and multimodal inputs including uploading charts, drawing sketches, and typing text. Textual responses to user queries are also displayed in the Chat Box. The responses are also connected to Main View, where the corresponding visualization reference is highlighted. Pattern View presents groups of typical data change patterns for the variable selected in Main View. These groups are ordered from top to bottom, with the most populated data change pattern at the top, tapering to the least at the bottom. Users can select a specific group of data change patterns, and then the top-3 visualization references of this pattern will be overlaid by highlighting the background. If there is an overlap among the displayed visualization references, the overlapping area corresponds to a darker background color. For users wishing to delve into each reference in detail, users can click the ‘show’ button located in the upper right corner of the Main View to achieve a circular review of each one. Additionally, Pattern View provides multimodal information (description text, different chart types, and candidate sketches) for a single variable’s typical change patterns, including descriptive text, various charts, and potential sketch candidates.

## 6 EVALUATION

To thoroughly evaluate *VisTR*, we conduct both quantitative evaluations and case studies. In the quantitative evaluations (Sect. 6.1), we assess the alignment ability of our fine-tuned MLLM. Subsequently, we present two cases on actual application scenarios (Sects. 6.2 & 6.3), representing a possible pathway through multimodal interactions to complete a time-series table reasoning task.

### 6.1 Effectiveness of Multimodal Visualization Alignment

We evaluate the alignment performance of our multimodal visualization alignment model from two perspectives: quantitative evaluation on text-chart retrieval, and user recognition on sketch-chart retrieval.

#### 6.1.1 Baselines and Metrics

We compare our fine-tuned MLLM against several pre-trained models: CLIP [48], OpenCLIP [10], and UniChart [43]. Our MLLM is a fine-tuned CLIP model on the composite dataset. To highlight the necessity and impact of the fine-tuning process, we compare it with the zero-shot CLIP and OpenCLIP models as an ablation study. Additionally, we validate the effectiveness of our fine-tuned CLIP by comparing it

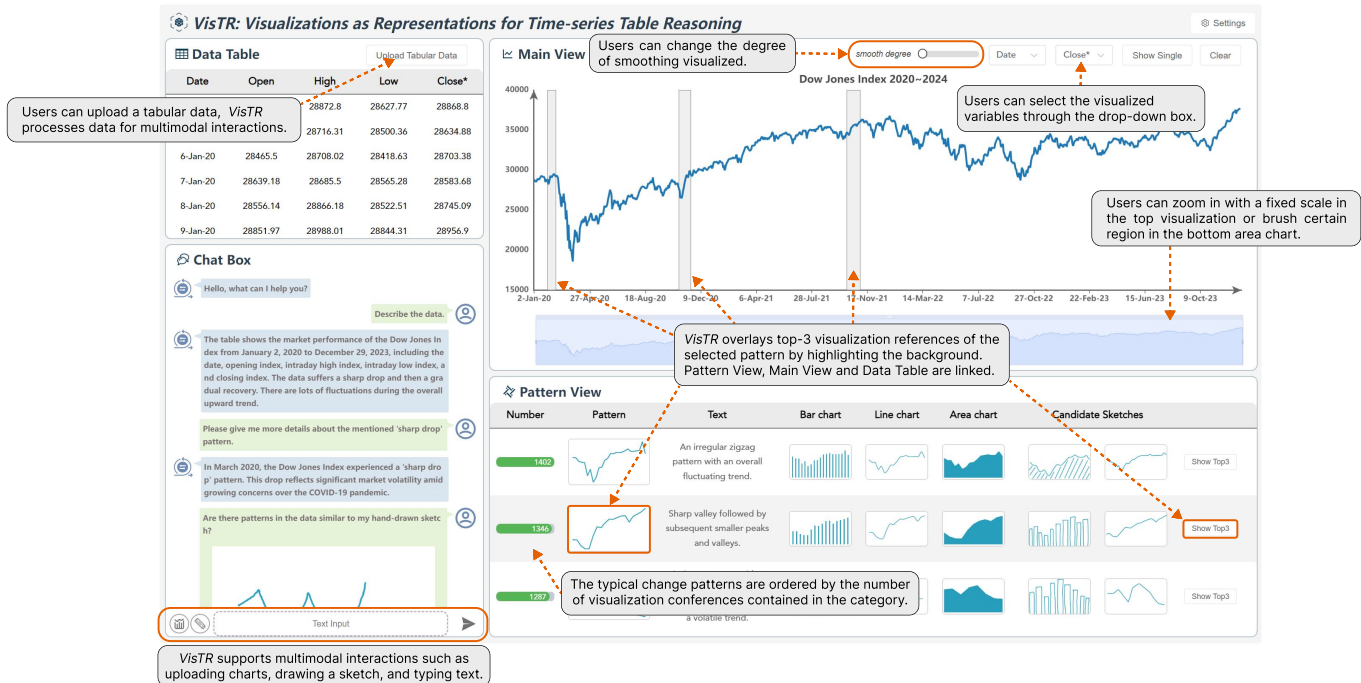


Fig. 7: The interactive interface of *VisTR*, which contains four main views and supports multimodal interactions for table reasoning.

Table 1: Experimental results on chart-to-text retrieval test for all and individual chart types.

Model		All	Bar	Line	Area
Ours	Acc (%)	<b>89.02</b>	<b>86.29</b>	<b>89.00</b>	<b>89.12</b>
(Fine-tuned CLIP)	WF (%)	<b>87.45</b>	<b>85.91</b>	<b>86.54</b>	<b>87.79</b>
Fine-tuned	Acc (%)	50.74	50.36	51.86	50.24
OpenCLIP	WF (%)	49.77	48.04	46.41	49.73
Zero-shot	Acc (%)	0.82	1.10	0.72	1.02
CLIP	WF (%)	0.36	0.29	0.11	0.07
Zero-shot	Acc (%)	7.71	8.20	5.27	1.08
OpenCLIP	WF (%)	5.37	3.78	1.95	0.30

against OpenCLIP and Unichart, confirming the appropriateness of our model selection. *VisTR* enables comprehensive multimodal binding among different modalities, rather than performing direct subsequence or sketch matching. In this sense, we omit the comparison with existing sketch query [17, 41] or sequence matching systems [21, 67].

Considering the imbalance among different trend word categories, we set two metrics for a comprehensive evaluation:

- Top-1 Accuracy (Acc). The accuracy calculates the ratio of true accurately identified pairs to the total number of pairs examined.
- Weighted F1-Score (WF). WF adopts the weighted average considering the unevenness of the categories, which is calculated as:  $WF = \frac{1}{T_N} \sum_{i=1}^{T_N} \frac{2 \times P_i \times R_i}{(P_i + R_i)}$ , where  $R_i$  and  $P_i$  are the recall and precision of the  $i^{th}$  trend-word category, respectively.

### 6.1.2 Text-Chart Retrieval

To rigorously assess the performance of our fine-tuned visualization alignment model in aligning chart-text pairs, we ensure that the evaluation dataset includes chart types of bar, line, and area chart, as well as all  $T_N = 23$  categories of trend words. Specifically, we randomly select 20% of the data for each chart type and each trend category from the chart-text pairing dataset for evaluation.

**Results.** The quantitative results are presented in Table 1. Our fine-tuned MLLM demonstrates robust performance in aligning chart and text modalities, with overall accuracy and weighted F1-score exceeding 85% across all chart types. The results for each individual chart type also provide substantial evidence of the model's effectiveness across various chart types. However, we observed that bar charts yield slightly



Fig. 8: Ratings of the visual similarity between pairs of the matched sketches and charts across our fine-tuned MLLM and three pre-trained models based on a 5-point Likert scale.

lower metrics than other chart types. This discrepancy may be attributed to the inherent characteristics of bar charts, which utilize separated bars to encode data, resulting in less distinctiveness compared to the continuous line marks used in line charts and the filled area marks used in area charts. To enhance the accuracy of bar charts, factors such as bar widths may need to be considered during fine-tuning process.

The comparisons between fine-tuned CLIP and zero-shot CLIP models confirm that fine-tuning is crucial for enhancing model performance in our specific domain. While zero-shot OpenCLIP slightly outperforms zero-shot CLIP, fine-tuned CLIP significantly surpasses fine-tuned OpenCLIP. Zero-shot OpenCLIP outperforms zero-shot CLIP is probably due to more extensive pre-training data that include more diverse chart images. However, after fine-tuning, CLIP's architecture process is better suited for our specific requirements. Its superior results validate our choice of CLIP as the base model.

### 6.1.3 Sketch-Chart Retrieval

We validate the alignment for chart-sketch pairs through a user study. Initially, we randomly selected 200 sketches from the chart-sketch dataset. Then, we tasked each of the four models (ours, CLIP, OpenCLIP, and UniChart) with determining the closest chart in the intent space to each selected sketch, indicating the chart with the highest similarity. This process constructed 800 matched sketch-chart pairings for the subsequent user study. We recruited 30 participants (15 women, and 15 men) with experience in building charts. Each participant is randomly given 20 sketches with their matched charts by each model and asked to rate the similarity between pairs of matched sketches and charts for each model, based on their visual perception of the correspondences. The ratings are gathered using a 5-point Likert scale [27], which provides a quantitative measure of the user agreement or disagreement with the similarities of chart-sketch pairs.

As shown in Figure 8, our model achieved the highest similarity agreement among participants (Mean = 4.33, SD = 0.67), and the Unichart achieved the lowest agreement with Mean = 2.25 and SD = 1.17. Given the non-normal distribution of collected ratings, we initiated our analysis by conducting the *Friedman test* to evaluate the statistical significance of ratings among the four models. The p-value of the *Friedman test* is less than 0.01, indicating significant differences between models. To further pinpoint the specific differences among models, we employed the *Wilcoxon signed-rank test* for paired comparisons, accompanied by *Bonferroni correction* to control errors. The pairwise comparisons showed that our model significantly outperformed the others. The detailed comparison results are shown in Figure 8. The poor performance of UniChart may be due to its focus on OCR features rather than chart features, leading to a weaker grasp of the varied patterns present within charts and hand-drawn sketches. The comparison results underscore the importance of encoding patterns in our alignment model, confirm the judicious choice of CLIP-ViT as our base pre-trained model, and highlight the superiority of our fine-tuned model in binding sketch and chart modalities.

## 6.2 Case Study 1: Financial Data Exploration

In this case, we consider a financial data exploration scenario. A market analyst, Mike, is studying the Dow Jones Index (DJI.)’s change patterns post-COVID-19. The used data measures the daily price movements of 30 large US companies, spanning from January 2nd, 2020 to December 29th, 2023. The data includes five columns: Date, Open, High, Low, and Close, detailing the trading metrics for each business day. Mike first loads the DJI. data into *VisTR* and selects ‘Close’ as the displayed variable in the Main View. *VisTR* initially generates 64,261 visualization references, among which 13,823 visualizations are pruned for exploration. The average retrieval time for querying a visualization reference stored in Chroma is within 0.6s.

As shown in Figure 9, Mike explores the data as follows.

- **Table Summarization.** Mike first enters the dialogue box “Describe the data.”. The response from *VisTR* includes two parts, one is the basic table description “The table shows the market performance of the Dow Jones Index from January 2, 2020, to December 29, 2023, including the date, opening index, intraday high index, intraday low index, and closing index.”, and the other is the overall trend description “The data suffers a sharp drop and then a gradual recovery. There are lots of fluctuations during the overall upward trend.”.
- **Question & Answering.** Given this description, Mike is interested in the “sharp drop” pattern, so he tries to locate the pattern by entering the text “Please give me more details about the mentioned ‘sharp drop’ pattern.”. Based on the context, *VisTR* can easily locate the “sharp drop” pattern that appears, and the matched interval is highlighted in Main View. At the same time, a text description “In March 2020, the Dow Jones Index experienced a ‘sharp drop’ pattern. This drop reflects significant market volatility amid growing concerns over the COVID-19 pandemic.” is returned in the dialogue box.
- **Visual Query.** Mike then freely sketches a ‘w’ pattern  in the empty canvas and enters “Are there patterns in the data similar to my hand-drawn sketch?”. *VisTR* retrievals for the visualization references similar to the input hand-drawn sketch from the vector database, and returns the three most similar matches in Main View. To facilitate user understanding, *VisTR* also returns a text description of the matched results: “The three intervals with similar patterns are from 8-Feb-21 to 16-Mar-21, 18-Feb-21 to 18-Mar-21, and 15-Dec-20 to 11-Jan-21. This pattern is recognized as a double-bottom pattern. It occurred in December 2020 and February 2021 suggesting that during both periods, the market demonstrated buyer interest at lower price levels after experiencing declines. This support prevented further downward movement. Higher prices prompted more buyers to participate, contributing to the Dow’s upward momentum.”.

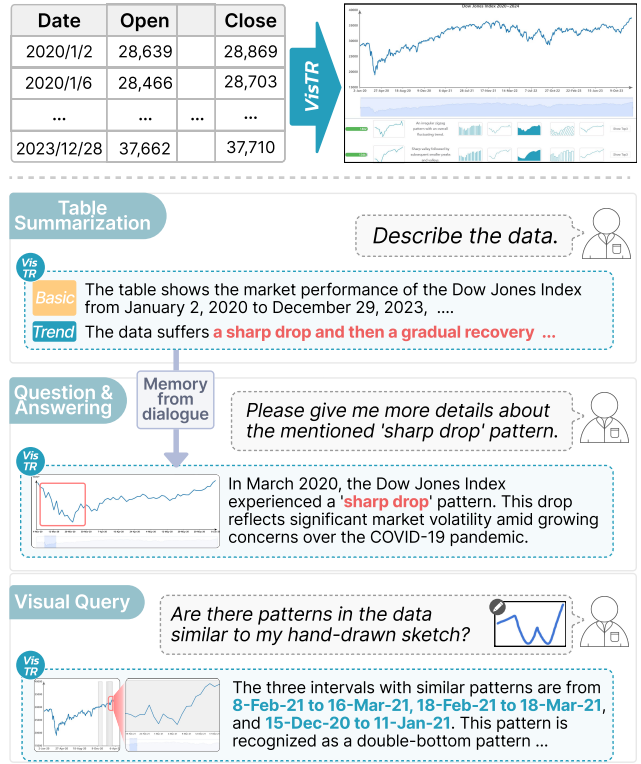


Fig. 9: Case study 1: data exploration for DJI. form 2020 to 2023. Mike gets a complete understanding of the data via table summarization, question & answering, and visual query enabled by *VisTR*.

In this way, Mike gets an overall understanding of the tabular data, and also typical trends and patterns within the data. The multimodal interactions, together with visual interactions like selecting and zooming in the visual interface, enable Mike to easily understand the DJI. data and recognize interesting data change patterns.

## 6.3 Case Study 2: Air Pollutant Analysis

In the second case, we demonstrate the workflow of mining relationships between data change patterns of different variables. A student, Emily, is seeking the correlations between different air pollutants. The used air pollutant dataset includes the daily air quality metrics from January 1, 2017, to December 31, 2018, which is collected by the Beijing US Embassy<sup>1</sup>. The data includes variables of Date, PM25, O3, temperature, and relative humidity, which provides insights into the fluctuations in air quality and correlations between air pollutants. Emily first loads the pollutant data into *VisTR*, which generates a multi-line chart with each line representing a variable. In the backend, *VisTR* generates a total of 102,787 visualization references, of which 40,243 are stored in Chroma after pruning.

Figure 10 illustrates Emily’s analysis process using *VisTR* to explore the multivariate data.

- **Free Exploration.** To obtain the typical data change patterns of pollutants, Emily selects four pollutant indicators, *PM25*, *O3*, *temperature*, and *relative humidity*, and obtains the change patterns in the Pattern View. She notices that all four indicators exhibit obvious daily fluctuations. Specifically, *PM25* exhibits a ‘zigzag pattern with varying amplitudes.’, indicative of its dynamic nature and daily variability. Similarly, a typical pattern of *O3* is ‘An irregular zigzag pattern with an overall fluctuating trend.’, further highlighting the pronounced daily jitters in pollutant levels. These observations motivate Emily to explore the relationship between these pollutant indicators over a long time interval.
- **Correlation Identification.** Different indicators have different data ranges, making it difficult to directly observe the relation-

<sup>1</sup><https://aqicn.org/city/beijing/us-embassy/cn/>

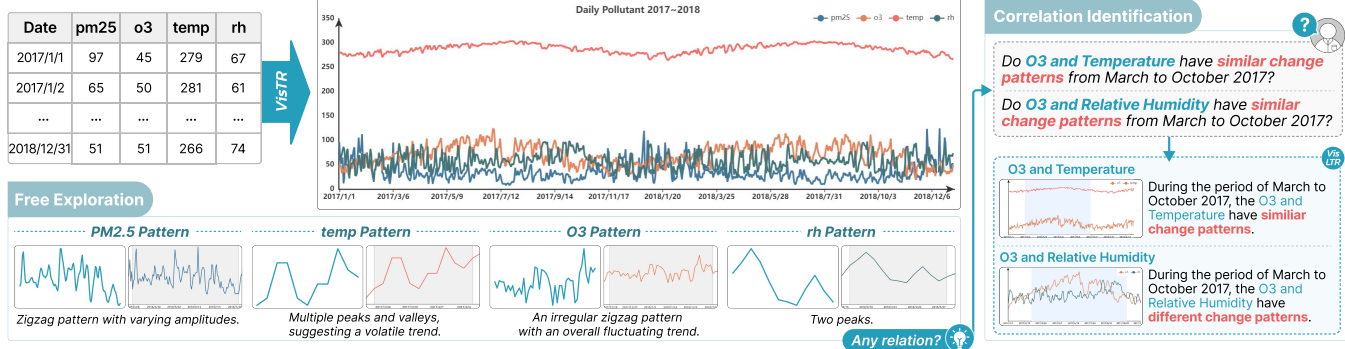


Fig. 10: Case study 2: multivariate analysis for the uploaded air pollutant dataset. With *VisTR*, Emily recognizes typical data change patterns and relationships between different air pollutants.

ships between different indicators in the Main View. For instance, the value of temperature is always greater than 250 (K), while the value of O3 hovers around 50 ( $\mu\text{g m}^{-3}$ ). To examine the correlation of these indicators, Emily chooses to directly raise questions to *VisTR* in the Chat Box. She enters “Do O3 and temperature have similar change patterns from March to October 2017?”. The O3 and temperature data change patterns during this period are highlighted in Main View and the response by *VisTR* is returned in the dialogue box: “During the period of March to October 2017, the O3 and Temperature have similar change patterns.”, and the response indicates a similar pattern between the indicators during the period. Emily further asks about the relationship between O3 and relative humidity, by entering “Do O3 and Relative Humidity have similar change patterns from March to October 2017?”. From the response, Emily can understand the data change patterns of O3 and relative humidity are different.

In this manner, Emily gains a comprehensive insight into the multivariate air pollutant data, recognizing both the typical data change patterns and correlations among various air pollutant indicators.

## 7 DISCUSSION

The case studies have demonstrated *VisTR*'s capability in recognizing and explaining data change patterns within tabular data. By leveraging visualizations as representation, *VisTR* successfully addresses the limitations of existing LLM-based table reasoning methods in pattern recognition and visual-based pattern exploration. Moreover, the process also aligns with the exploratory data analysis (EDA) process. EDA often involves summarizing the main characteristics of a dataset using visualization, enabling users to understand the data's structure, recognize patterns, detect anomalies, and formulate hypotheses for further investigation. In this sense, the proposed framework not only streamlines the process of EDA but also expands its horizons, providing users with novel approaches to uncover hidden patterns within datasets.

**Generalizability.** Nevertheless, to fully realize the potential of the proposed framework, we need to enhance the generalizability of *VisTR* from the following perspectives.

- **More table types.** *VisTR* is currently instantiated on time-series tables, which contain data change patterns that cannot be processed by existing SQL-based LLMs for table reasoning. *VisTR* has the potential to be extended to more general table types by employing alternative data transformation methods within the *visualization referencing* module. For instance, *VisTR* can be adapted to recognize and analyze the distribution patterns in a student grade table. In this scenario, a data aggregation method could be employed to recognize grade distribution patterns, such as the normal distribution. Supporting a broader range of table types is feasible, leveraging methods such as subset embedding [62] and learning-based approaches [54].
- **General user queries.** *VisTR* focuses on tasks related to reasoning about data change patterns in tables. Therefore, we primarily provide text-based user queries related to data change patterns, such as “what type of change pattern exists in the data?” However, this narrow

focus also limits our ability to handle other general user queries, including those related to causal reasoning, such as “why did Apple stock rise in March?” When posed with such questions, *VisTR* may encounter the ‘hallucination’ issue, leading to incorrect queries and responses. To achieve a comprehensive exploration and reasoning of a data table, we require more general user queries, which may necessitate the incorporation of external knowledge sources.

- **Intent-enhanced sketches.** Users’ intuition about sketching targets often emerges from the exploration process. As a reason, *VisTR* offers insights into common patterns within the uploaded table. However, expressing complex and less common patterns solely through hand-drawn sketches can be challenging for users [32]. To address this challenge, several solutions can be considered. First, incorporating additional interactive features such as dragging, resizing, and erasing, sketches can provide users with greater flexibility in adjusting their intent [36]. Summarizing multi-attribute temporal patterns and introducing a more effective time-series segmentation method have shown promise in addressing this issue [51]. By implementing these methods, we can further enhance the capabilities of *VisTR* to support sketches with enhanced intents.

**Scaling up the dataset.** The successful alignment of our model heavily relies on acquiring high-quality training data. Scaling up the dataset to enhance the generalizability of *VisTR* presents significant challenges for the data augmentation and user labeling strategies currently employed. Collecting user-labeled sketches is time-consuming, and incorporating intents into sketches would further increase complexity. To address this limitation, one solution is to leverage crowdsourcing strategies, although this still requires significant manual effort. Another innovative technique would be to use large models to simulate and augment a variety of hand-drawn patterns. LLM-powered data augmentation has been a promising direction [11], and we are interested in using this approach for scaling up the dataset.

**Potential scenarios.** Besides table reasoning, the proposed framework holds potential for other application scenarios, such as safeguarding sensitive data that requires a balance between data privacy and utility. By transforming raw tabular data into visualizations, *VisTR* shields the secure information contained within tables from users, while still allowing for examination and querying of the data patterns. Moreover, *VisTR* could also find applications in fraud detection, as visualizations generated from transactional data could help recognize suspicious patterns indicative of fraudulent activities.

## 8 CONCLUSION

This work introduces *VisTR* system, built upon a novel framework for table reasoning, expanding upon existing LLM-based table reasoning research. By leveraging visualizations as *representations*, the framework offers several advantages, including the ability to recognize data change patterns, mitigate LLM drift, and support visual-based exploration. The implementation of *VisTR* requires an effective multimodal visualization alignment model that binds chart, text, and sketch modalities together in a joint embedding space. This is accomplished by

fine-tuning an MLLM with a new dataset of chart-text and chart-sketch pairings. Combined with strategies employed for visualization referencing, indexing, and pruning, we have developed an interactive system that facilitates multimodal interactions with time-series tables. The feasibility of *VisTR* is demonstrated through quantitative evaluations of the visualization alignment model and practical case studies on time-series data tables. This proposed framework offers a new research direction for table reasoning and enhances the fuzzy exploration process of existing LLM-based table reasoning methods. We aim to extend its support to a wider range of table types, accommodate more generalized user queries, and explore additional application scenarios in the future.

## ACKNOWLEDGMENTS

## REFERENCES

- [1] Chroma. <https://www.trychroma.com/>. Accessed: 2024-03-20. 3, 6
- [2] Euclidesdb. <https://euclidesdb.readthedocs.io/en/latest/>. Accessed: 2024-03-20. 3
- [3] A. Asai, S. Min, Z. Zhong, and D. Chen. Retrieval-based Language Models and Applications. In *Proc. ACL*, pp. 41–46, 2023. 3
- [4] L. Chen, M. Zaharia, and J. Zou. How is ChatGPT’s Behavior Changing over Time? *arXiv preprint arXiv:2307.09009*, 2023. 1, 2
- [5] W. Chen. Large Language Models are few(1)-shot Table Reasoners. In *Proc. EACL*, pp. 1090–1100, 2023. 1, 2
- [6] W. Chen, H. Wang, J. Chen, Y. Zhang, H. Wang, S. Li, X. Zhou, and W. Y. Wang. TabFact: A Large-scale Dataset for Table-based Fact Verification. In *Proc. ICLR*, 2020. 1, 2
- [7] W. Chen, H. Wang, J. Chen, Y. Zhang, H. Wang, S. Li, X. Zhou, and W. Y. Wang. TabFact: A Large-scale Dataset for Table-based Fact Verification. In *Proc. ICLR*, 2020. 6
- [8] Y. Chen, M. A. Nascimento, B. C. Ooi, and A. K. Tung. Spade: On shape-based pattern detection in streaming time series. In *Proc. IEEE ICDE*, pp. 786–795. IEEE, 2006. 1
- [9] Z. Cheng, T. Xie, P. Shi, C. Li, R. Nadkarni, Y. Hu, C. Xiong, D. Radev, M. Ostendorf, L. Zettlemoyer, N. A. Smith, and T. Yu. Binding Language Models in Symbolic Languages. In *Proc. ICLR*, 2023. 1
- [10] M. Cherti, R. Beaumont, R. Wightman, M. Wortsman, G. Ilharco, C. Gordon, C. Schuhmann, L. Schmidt, and J. Jitsev. Reproducible Scaling Laws for Contrastive Language-Image Learning. In *Proc. CVPR*, pp. 2818–2829, 2023. 6
- [11] B. Ding, C. Qin, R. Zhao, T. Luo, X. Li, G. Chen, W. Xia, J. Hu, A. T. Luu, and S. Joty. Data Augmentation using LLMs: Data Perspectives, Learning Paradigms and Challenges. In *Proc. ACL*, pp. 1679–1705, 2024. 9
- [12] H. Dong and Z. Wang. Large Language Models for Tabular Data: Progresses and Future Directions. In *Proc. ACM SIGIR*, pp. 2997–3000, 2024. 1
- [13] A. Dosovitskiy, L. Beyer, A. Kolesnikov, D. Weissenborn, X. Zhai, T. Unterthiner, M. Dehghani, M. Minderer, G. Heigold, S. Gelly, J. Uszkoreit, and N. Houlsby. An image is worth 16x16 words: Transformers for image recognition at scale. In *Proc. ICLR*, 2021. 3, 4
- [14] J. M. Eisenschlos, S. Krichene, and T. Müller. Understanding tables with intermediate pre-training. In *Proc. EMNLP*, vol. EMNLP 2020, pp. 281–296, 2020. 2
- [15] M. Eitz, J. Hays, and M. Alexa. How Do Humans Sketch Objects? *ACM Trans. Graph.*, 31(4):44:1–44:10, 2012. 4
- [16] F. Faghri, D. J. Fleet, J. R. Kiros, and S. Fidler. VSE++: Improving Visual-Semantic Embeddings with Hard Negatives. In *Proc. BMVC*, p. 12, 2018. 4
- [17] C. Fan, K. Matković, and H. Hauser. Sketch-based fast and accurate querying of time series using parameter-sharing LSTM networks. *IEEE Trans. Vis. Comput. Graph.*, 27(12):4495–4506, 2020. 7
- [18] S. Few. Show me the numbers. *Analytics Pres*, 2004. 2
- [19] L. Gao, A. Madaan, S. Zhou, U. Alon, P. Liu, Y. Yang, J. Callan, and G. Neubig. PAL: Program-aided Language Models. In *Proc. IEEE ICML*, vol. 202, pp. 10764–10799, 2023. 1
- [20] R. Girdhar, A. El-Nouby, Z. Liu, M. Singh, K. V. Alwala, A. Joulin, and I. Misra. Imagebind: One Embedding Space to Bind Them All. In *Proc. CVPR*, pp. 15180–15190, 2023. 3, 5
- [21] A. Gogolou, T. Tsandilas, T. Palpanas, and A. Bezerianos. Comparing Similarity Perception in Time Series Visualizations. *IEEE Trans. Vis. Comput. Graph.*, 25(1):523–533, 2019. 7
- [22] R. Guo, X. Luan, L. Xiang, X. Yan, X. Yi, J. Luo, Q. Cheng, W. Xu, J. Luo, F. Liu, Z. Cao, Y. Qiao, T. Wang, B. Tang, and C. Xie. Manu: A Cloud Native Vector Database Management System. *Proc. VLDB*, 15(12):3548–3561, 2022. 3
- [23] J. Hao, Q. Shi, Y. Ye, and W. Zeng. TimeTuner: Diagnosing Time Representations for Time-Series Forecasting with Counterfactual Explanations. *IEEE Trans. Vis. Comput. Graph.*, 2023. 5
- [24] E. Hoque, P. Kavehzadeh, and A. Masry. Chart Question Answering: State of the art and future directions. *Comput. Graph. Forum*, 41(3):555–572, 2022. 2
- [25] Z. Jiang, Y. Mao, P. He, G. Neubig, and W. Chen. OmniTab: Pretraining with natural and synthetic data for few-shot table-based question answering. *arXiv preprint arXiv:2207.03637*, 2022. 2
- [26] N. Jin, J. Siebert, D. Li, and Q. Chen. A Survey on Table Question Answering: Recent Advances. In *Proc. CCKS*, vol. 1669, pp. 174–186, 2022. 1, 2
- [27] A. Joshi, S. Kale, S. Chandel, and D. K. Pal. Likert Scale: Explored and explained. *BJAST*, 7(4):396–403, 2015. 7
- [28] S. Kantharaj, R. T. K. Leong, X. Lin, A. Masry, M. Thakkar, E. Hoque, and S. R. Joty. Chart-to-Text: A Large-Scale Benchmark for Chart Summarization. In *Proc. ACL*, pp. 4005–4023, 2022. 3, 4
- [29] H. Kim, B.-H. So, W.-S. Han, and H. Lee. Natural language to SQL: Where are we today? *Proc. VLDB*, 13(10):1737–1750, 14 pages, jun 2020. 2
- [30] T. Kojima, S. S. Gu, M. Reid, Y. Matsuo, and Y. Iwasawa. Large Language Models are Zero-Shot Reasoners. In *Proc. NeurIPS*, 2022. 2
- [31] A. Lazard and L. Atkinson. Putting environmental infographics center stage: The role of visuals at the elaboration likelihood model’s critical point of persuasion. *Science Communication*, 37(1):6–33, 2015. 2
- [32] D. J.-L. Lee, J. Lee, T. Siddiqui, J. Kim, K. Karahalios, and A. Parameswaran. You can’t always sketch what you want: Understanding Sensemaking in Visual Query Systems. *IEEE Trans. Vis. Comput. Graph.*, 26(1), 2020. 2, 9
- [33] F. Lekschas, B. Peterson, D. Haehn, E. Ma, N. Gehlenborg, and H. Pfister. Peax: Interactive Visual Pattern Search in Sequential Data Using Unsupervised Deep Representation Learning. *Comput. Graph. Forum*, 39(3):167–179, 2020. 3
- [34] Z. Li, Q. Ke, and W. Chen. CLIP Guided Image-perceptive Prompt Learning for Image Enhancement. *arXiv preprint arXiv:2311.03943*, 2023. 2
- [35] J. Lin, S. Williamson, K. Borne, and D. DeBarr. Pattern recognition in time series. *Advances in Machine Learning and Data Mining for Astronomy*, 1(617-645):3, 2012. 1
- [36] Y. Lin, H. Li, L. Yang, A. Wu, and H. Qu. InkSight: Leveraging sketch interaction for documenting chart findings in computational notebooks. *IEEE Trans. Vis. Comput. Graph.*, 2023. 9
- [37] Q. Liu, B. Chen, J. Guo, M. Ziyadi, Z. Lin, W. Chen, and J. Lou. TAPEX: Table Pre-training via Learning a Neural SQL Executor. In *Proc. ICLR*, 2022. 2
- [38] Y. Luo, Y. Zhou, N. Tang, G. Li, C. Chai, and L. Shen. Learned Data-aware Image Representations of Line Charts for Similarity Search. *Proc. ACMMOD*, 1(1):1–29, 2023. 3
- [39] R. Ma, H. Mei, H. Guan, W. Huang, F. Zhang, C. Xin, W. Dai, X. Wen, and W. Chen. LADV: Deep Learning Assisted Authoring of Dashboard Visualizations From Images and Sketches. *IEEE Trans. Vis. Comput. Graph.*, 27(9):3717–3732, 2020. 4
- [40] Y. Ma, A. K. Tung, W. Wang, X. Gao, Z. Pan, and W. Chen. ScatterNet: A deep subjective similarity model for visual analysis of scatterplots. *IEEE Trans. Vis. Comput. Graph.*, 26(3):1562–1576, 2018. 3
- [41] M. Mannino and A. Abouzied. Expressive time series querying with hand-drawn scale-free sketches. In *Proc. ACM CHI*, pp. 1–13, 2018. 1, 3, 4, 7
- [42] A. Masry, X. L. Do, J. Q. Tan, S. Joty, and E. Hoque. ChartQA: A Benchmark for Question Answering about Charts with Visual and Logical Reasoning. In *Proc. ACL*, pp. 2263–2279, 2022. 2, 3
- [43] A. Masry, P. Kavehzadeh, X. L. Do, E. Hoque, and S. Joty. Unichart: A Universal Vision-language Pretrained Model for Chart Comprehension and Reasoning. *arXiv preprint arXiv:2305.14761*, 2023. 2, 6
- [44] H. Mouss, D. Mouss, N. Mouss, and L. Sefouhi. Test of Page-Hinckley, an approach for fault detection in an agro-alimentary production system. In *Proc. IEEE ASCC*, vol. 2, pp. 815–818, 2004. 5
- [45] M. E. Newman. Power laws, Pareto distributions and Zipf’s law. *Contemporary Physics*, 46(5):323–351, 2005. 6

- [46] J. J. Pan, J. Wang, and G. Li. Survey of vector database management systems. *Proc. VLDB*, pp. 1–25, 2024. 3
- [47] B. Qin, B. Hui, L. Wang, M. Yang, J. Li, B. Li, R. Geng, R. Cao, J. Sun, L. Si, et al. A survey on text-to-sql parsing: Concepts, methods, and future directions. *arXiv preprint arXiv:2208.13629*, 2022. 6
- [48] A. Radford, J. W. Kim, C. Hallacy, A. Ramesh, G. Goh, S. Agarwal, G. Sastry, A. Askell, P. Mishkin, J. Clark, G. Krueger, and I. Sutskever. Learning Transferable Visual Models From Natural Language Supervision. In *Proc. IEEE ICML*, vol. 139, pp. 8748–8763, 2021. 2, 3, 4, 6
- [49] A. Radford, J. Wu, R. Child, D. Luan, D. Amodei, I. Sutskever, et al. Language models are unsupervised multitask learners. *OpenAI blog*, 1(8):9, 2019. 3, 4
- [50] V. Schetinger, S. Di Bartolomeo, M. El-Assady, A. McNutt, M. Miller, J. P. A. Passos, and J. L. Adams. Doom or Deliciousness: Challenges and Opportunities for Visualization in the Age of Generative Models. *Comput. Graph. Forum*, 42(3):423–435, 2023. 2
- [51] G. Shirato, N. Andrienko, and G. Andrienko. Identifying, exploring, and interpreting time series shapes in multivariate time intervals. *Visual Informatics*, 7(1):77–91, 2023. 9
- [52] T. Siddiqui, J. Lee, A. Kim, E. Xue, X. Yu, S. Zou, L. Guo, C. Liu, C. Wang, K. Karahalios, et al. Fast-Forwarding to Desired Visualizations with Zenvisage. In *Proc. CIDR*, 2017. 3
- [53] J. S. Simonoff. *Smoothing methods in statistics*. Springer Science & Business Media, 2012. 5
- [54] Y. Sun, J. Li, S. Chen, G. Andrienko, N. Andrienko, and K. Zhang. A learning-based approach for efficient visualization construction. *Visual Informatics*, 6(1):14–25, 2022. 2, 9
- [55] J. Wang, X. Yi, R. Guo, H. Jin, P. Xu, S. Li, X. Wang, X. Guo, C. Li, X. Xu, K. Yu, Y. Yuan, Y. Zou, J. Long, Y. Cai, Z. Li, Z. Zhang, Y. Mo, J. Gu, R. Jiang, Y. Wei, and C. Xie. Milvus: A Purpose-Built Vector Data Management System. In *Proc. ACM SIGMOD*, pp. 2614–2627, 2021. 3
- [56] L. Wang, B. Qin, B. Hui, B. Li, M. Yang, B. Wang, B. Li, J. Sun, F. Huang, L. Si, et al. PROTON: Probing Schema Linking Information from Pre-trained Language Models for Text-to-SQL Parsing. In *Proc. ACM KDD*, pp. 1889–1898, 2022. 2, 6
- [57] Z. Wang, H. Zhang, C. Li, J. M. Eisenschlos, V. Perot, Z. Wang, L. Miculich, Y. Fujii, J. Shang, C. Lee, and T. Pfister. Chain-of-Table: Evolving Tables in the Reasoning Chain for Table Understanding. In *Proc. ICLR*, 2024. 1, 2
- [58] C. Wei, B. Wu, S. Wang, R. Lou, C. Zhan, F. Li, and Y. Cai. AnalyticDB-V: A Hybrid Analytical Engine Towards Query Fusion for Structured and Unstructured Data. *Proc. VLDB*, 13(12):3152–3165, 2020. 3
- [59] R. Xia, B. Zhang, H. Peng, N. Liao, P. Ye, B. Shi, J. Yan, and Y. Qiao. Structchart: Perception, structuring, reasoning for visual chart understanding. *arXiv preprint arXiv:2309.11268*, 2023. 4
- [60] S. Xiao, Y. Hou, C. Jin, and W. Zeng. WYTIWYR: A User Intent-Aware Framework with Multi-modal Inputs for Visualization Retrieval. *Comput. Graph. Forum*, 42(3):311–322, 2023. 2
- [61] S. Xiao, S. Huang, Y. LIN, Y. Ye, and W. Zeng. Let the Chart Spark: Embedding Semantic Context into Chart with Generative Model. *IEEE Trans. Vis. Comput. Graph.*, 30(1):284–294, 2024. 2
- [62] P. Xie, W. Tao, J. Li, W. Huang, and S. Chen. Exploring Multi-dimensional Data via Subset embedding. *Comput. Graph. Forum*, 40(3):75–86, 2021. 2, 5, 9
- [63] Y. Ye, J. Hao, Y. Hou, Z. Wang, S. Xiao, Y. Luo, and W. Zeng. Generative AI for visualization: State of the art and future directions. *Visual Informatics*, 8(2):43–66, 2024. 1
- [64] Y. Ye, R. Huang, and W. Zeng. VISAtlas: An image-based Exploration and Query System for Large Visualization Collections via Neural Image Embedding. *IEEE Trans. Vis. Comput. Graph.*, 2022. 3, 4
- [65] Y. Ye, B. Hui, M. Yang, B. Li, F. Huang, and Y. Li. Large language models are versatile decomposers: Decomposing evidence and questions for table-based reasoning. In *Proc. ACM SIGIR*, pp. 174–184, 2023. 1, 2, 6
- [66] Y. Ye, B. Hui, M. Yang, B. Li, F. Huang, and Y. Li. Large Language Models are Versatile Decomposers: Decomposing Evidence and Questions for Table-based Reasoning. In *Proc. ACM SIGIR*, pp. 174–184, 2023. 2
- [67] Y. Yu, T. Becker, M. Behrisch, et al. SAXRegEx: Multivariate time series pattern search with symbolic representation, regular expression, and query expansion. *Comput. Graph.*, 112:13–21, 2023. 7
- [68] X. Zeng, H. Lin, Y. Ye, and W. Zeng. Advancing multimodal large language models in chart question answering with visualization-referenced instruction tuning. *IEEE Trans. Vis. Comput. Graph.*, pp. 1–11, 2024. 2
- [69] X. Zhang, D. Wang, L. Dou, B. Wang, D. Wu, Q. Zhu, and W. Che. FLEXTAF: Enhancing Table Reasoning with Flexible Tabular Formats. *arXiv preprint arXiv:2408.08841*, 2024. 1
- [70] X. Zhang, D. Wang, L. Dou, Q. Zhu, and W. Che. A Survey of Table Reasoning with Large Language Models. *arXiv preprint arXiv:2402.08259*, 2024. 1
- [71] C. Zhou, C. C. Loy, and B. Dai. Extract Free Dense Labels from CLIP. In *Proc. ECCV*, pp. 696–712, 2022. 2
- [72] X. Zhou, R. Girdhar, A. Joulin, P. Krähenbühl, and I. Misra. Detecting Twenty-thousand Classes using Image-level Supervision. In *Proc. ECCV*, pp. 350–368, 2022. 2